# Influence of Substrate Mechanical Properties on Lens Epithelial Cell Behavior

Undergraduate Thesis

Presented in Partial Fulfillment of the Requirements for the degree Bachelor of Science with Honors Research Distinction

By

Mallory Grace Allen

Department of Biomedical Engineering

The Ohio State University

2018

Committee:

Katelyn E. Swindle-Reilly, Ph.D., Advisor

Matthew A. Reilly, Ph.D.

## Abstract

Posterior capsular opacification (PCO), or secondary cataract, is the most common complication of after cataract surgery, but current clinical solutions are expensive, have complications, and are not available in developing countries. While PCO has been widely studied, little to no research exists to examine the link between mechanical properties of implanted intraocular lenses (IOLs) and occurrence of secondary cataract. The goal of this project was to start to close this scientific gap by measuring mechanical properties of a series of amphiphilic polymers and investigating their impact on lens epithelial cell (LEC) response. Polymers with different levels of crosslinking were synthesized to modulate mechanical stiffness. The unloading moduli of these polymers were measured by nanoindentation, but it did not provide any statistically significant data. Rheology was also used to quantify the mechanical properties of polymers. The storage moduli of polymers were in the range of 0.9-30 kPa, and the loss moduli of polymers were in the range of 0.1-35 kPa. Rheology data was somewhat inconsistent, so in the future, it is important to design rheology methods that provide more accurate data. Preliminary data showed that primary canine LECs seeded onto polymer films in a well plate tended to preferentially attach to stiffer surfaces. When polymers were seeded with human LECs, they tended to preferentially attach to polymers with a higher ratio of TRIS. However, there were no clear trends in the amount of cell attachment with changing degree of crosslinking. This study should be repeated with more replicates and multiple batches of

polymers. Further research will look to complete a comprehensive study of both chemical and mechanical properties of amphiphilic polymers so that optimal IOL properties can be determined to potentially prevent PCO. Additionally, the epithelial-mesenchymal transition of LECs on these surfaces will be investigated.

## Acknowledgments

I would like to thank my research mentor, Dr. Katelyn E. Swindle-Reilly, for all of her guidance and assistance on my project. She has been a great source of advice and encouragement during my time as an undergraduate researcher and has helped me develop problem solving skills and confidence that will surely help me in my career and life. I want to acknowledge Dr. Do-Gyoon Kim for providing me with the nanoindentation data and Dr. Heather Chandler for providing me with the preliminary data on the canine lens epithelial cells. I would also like to thank my lab mates; particularly Sophie Carus, Katrina Schroeder, and Ryan Prieto for their help with experiments and their ideas when I was stuck and didn't know what to do next. They have been my moral support and have made research lots of fun. I sincerely appreciate The Ohio State University College of Engineering for providing me with a research scholarship and the opportunity to publish an undergraduate thesis. I also would like to thank Andy Soltisz and Dr. Matthew A. Reilly for their guidance in my rheology testing and Dr. Alexis Ortiz-Rosario for help with statistics. Finally, I want to thank my family for their constant love and reassurance. My parents have provided me with the opportunity to attend The Ohio State University and have believed in me every step of the way, and my sisters have been by my side through every challenge and triumph. I am truly blessed to have an amazing support system.

## Vita

2014…….……Canfield High School, Canfield OH

2018……B.S. Biomedical Engineering, The Ohio State University

## Publications

Tram, N.K., Jiang, P., Allen, M., Prieto, R., Carus, S., Reilly, M.A., & Swindle-Reilly, K.E. (2018). The influences of accommodative tissues on corneal morphogenesis. (submitted).

## Fields of Study

Major Field: Biomedical Engineering

Minor Field: Integrative Approaches to Health and Wellness

Table of Contents

# List of Tables

# List of Figures

# Introduction

Cataract is opacification of the crystalline lens of the eye, which decreases light transmission, hindering effective vision. It is the leading cause of blindness worldwide (Tortolano et al, 2015). Studies have reported that the prevalence of cataract increases dramatically with age, "from 3.9% at age 55-64 years to 92.6% at age 80 years and older" (Liu et al., 2017). Currently, the only treatment option for cataract is surgery in which the opacified lens is removed through a hole in the lens capsule and a rigid synthetic intraocular lens (IOL) is implanted in its place. Approximately 3 million cataract surgeries are performed each year in the U.S. (Bertrand et. al. 2014).

During surgery, the clouded lens is extracted by phacoemulsification, a process in which the lens is broken up with ultrasound irradiation and then aspirated out of the lens capsule through a small hole (Tortolano et al, 2015). A foldable intraocular lens implant is inserted in place of the native lens. This surgical process can be visualized in Figure 1, below.

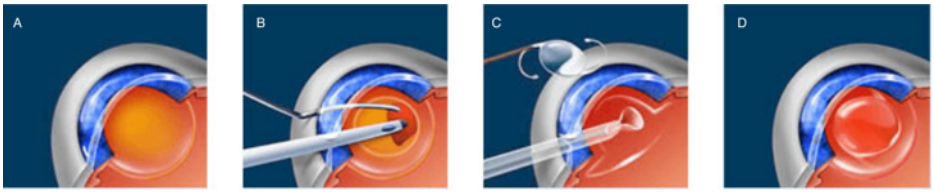


**Figure 1 : Animation showing steps of cataract surgery. A) Incision on cornea to access lens area. B) Ultrasound irradiation to break up crystalline lens. C) Aspiration of broken-up lens to make room for IOL. D) Insertion of IOL. (Source: Southwestern Eye Associates)**

While the surgical process is relatively streamlined, the specific intraocular lens inserted in each surgical case can differ. Most IOLs consist of a main circular optic piece with haptics extending out from the main body to help secure the lens in place. The haptic rigidity and memory are the two factors that can determine how well the implant will center after surgery. Some IOLs are designed in more of a plate shape without haptics. However, these plate style IOLs can cause complications because of their shape. Figure 2, below, shows different IOL designs that are currently used during cataract surgery.

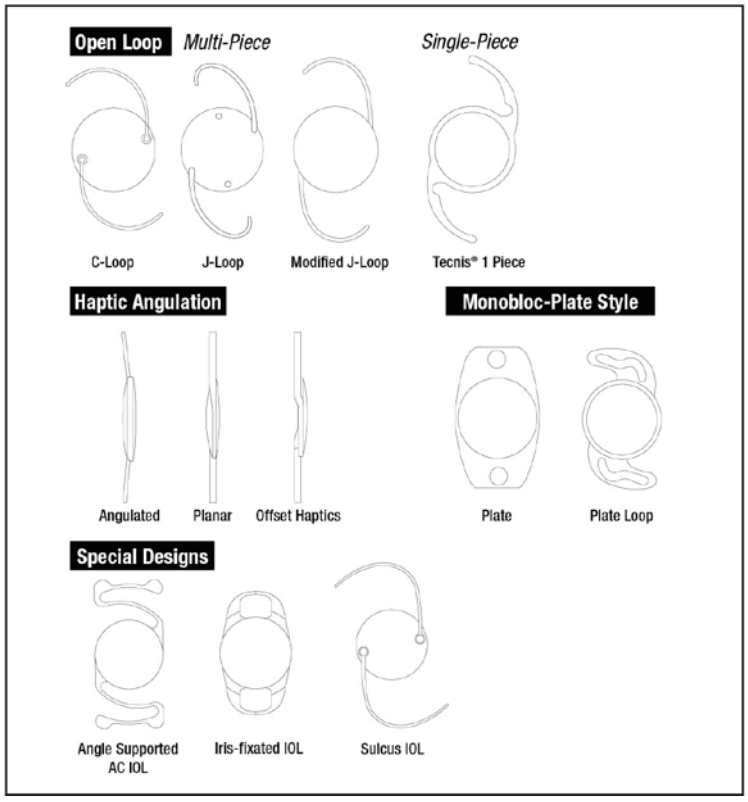


**Figure 2: IOL Design Types (Findl, 2009)**

The most common complication of cataract surgery is posterior capsular opacification (PCO), also known as secondary cataract. This process occurs when lens epithelial cells (LECs) migrate and attach onto the intraocular lens surface and then

proliferate and undergo epithelial-mesenchymal transition (EMT), causing the surface to become cloudy (Awasthi, Guo, & Wagner, 2009). Slitlamp photographs shown in Figure 3, below, show human eyes with posterior capsule opacification in different parts of the posterior capsule.

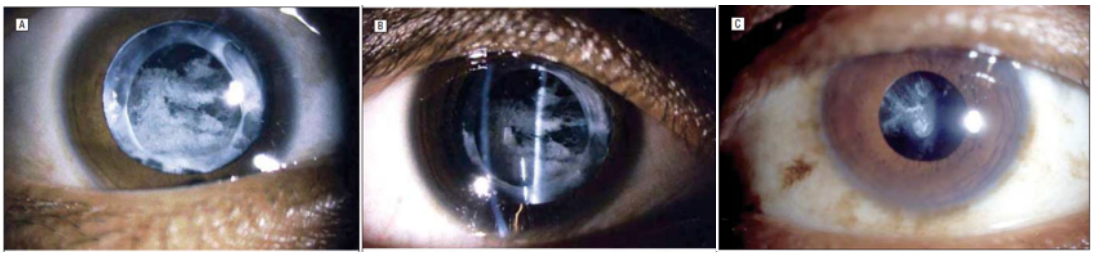

**Figure 3: Slitlamp photographs with different illumination and magnification representing PCO that is on different areas of the posterior capsule (Awasthi, Guo, & Wagner, 2009)**

PCO can occur in up to 50% of all patients who undergo cataract surgery 2-5 years after surgery, with a particularly high incidence occurring in pediatric patients (Princz et al., 2016).

Currently, posterior capsular opacification can be treated by Nd:YAG laser capsulotomy, but there are significant problems with this course of treatment. This surgery can cause further ocular problems such as increased intraocular pressure, ocular inflammation, retinal detachment, and cystoid macular edema. Additionally, it is expensive and not available in many developing countries (Findl, 2009). Overall, it is a supreme burden on the healthcare system when IOLs can be designed specifically to reduce the incidence of PCO (Hollick, Spalton, Ursell, Pande, Barman, Boyce, & Tilling, 1999). It is hypothesized that the need for capsulotomy should be lowered by using intraocular lenses with optimal properties for inhibiting lens epithelial cell adhesion and proliferation and thus, PCO (Princz, Lasowski, & Sheardown, 2016).

PCO has also been experimentally treated with drugs that prevent the migration and proliferation of LECs, but due to toxicity and side effects, they are not currently used for clinical treatment (Spalton 1999; Huang et al., 2013). Additionally, IOL design has been tested by changing the shape or edge design and by coating the IOL surface with different materials.

Oshika et al.'s (1998) study of adhesion of the lens capsule to intraocular lenses found that the edge of the IOL optics suppressed migration of lens epithelial cells to the posterior capsule's center. This finding led to other studies on the effect of edge design of intraocular lenses influencing PCO. It has been found that IOLs with sharp posterior optic edges can prevent PCO, and there is not a significant different in prevention between these IOLs, regardless of their material composition (Nishi, Nishi,& Osakabe, 2004). A 360 degree sharp edge design has also proven to be effective in preventing PCO (Menucci et al, 2015). Some of these sharp edge designs are shown in Figure 4, on the next page.


**Figure 4: IOLs used in the study by Nishi et al. 2004 with A, B, and C demonstrating different sharp edge designs and D as the blunt truncated edge control**

However, these edge designs need to be studied in long-term clinical evaluation to more accurately estimate their functional results. This is also true of IOL designs that coat the surface in materials such as PEG to prevent adhesion of lens epithelial cells (Xu et al, 2016). While these methods may prove to be effective in the future, they are still relatively new and may take years to become clinically relevant.

The choice intraocular lens biomaterial is quite likely the most influential factor in the occurrence of secondary cataract. Ursell et al. (1998) found that a copolymer of phenylethyl acrylate and phenylethyl methacrylate crosslinked with butanediol diacrylate (AcrySof®) had significantly less PCO than both poly(methyl methacrylate) (PMMA) and silicone. Versura et al. (1999) studied lens epithelial cell adhesion on a few different

intraocular lens materials and concluded that using IOL surfaces that discourage cell adhesion will reduce the incidence of PCO.

Further studies from other groups have tried to investigate why certain materials limit LEC adhesion and inhibit PCO more than others. Many have hypothesized that this difference is due to the hydrophobicity or hydrophilicity of the IOL material and most have concluded that hydrophilic lenses have significantly less cells adhered to the surface, but some studies have found conflicting results indicating that hydrophilic IOLs have more cells adhered to the surface (Cunanan et al, 1991; Kugelberg et al, 2008; Iwase et al, 2011). These conflicting results may suggest that other properties of the implant biomaterial are influencing the incidence of PCO.

While many studies on posterior capsular opacification have been done, there is a significant knowledge gap in how the mechanical properties of the IOL affect its occurrence. There have been no well-designed studies investigating this phenomenon (Princz, Lasowski, & Sheardown, 2016). A bottom-up approach must be taken to design IOLs with optimal properties for preventing PCO, but this cannot be done if the optimal properties are not known. This project aims to identify the optimal mechanical properties of a broad range of amphiphilic polymers for preventing lens epithelial cell attachment and proliferation in order to ultimately design IOLs to potentially prevent PCO.

The native lens capsule has an elastic modulus in the range of 0.4-1.5 MPa, (Krag & Andreassen, 2003). It has been hypothesized that the optimal mechanical properties of an intraocular lens implant should be lower than that of the native lens capsule. This is based off of literature reports that currently used IOLs are significantly more rigid than the lens capsule. The enVista IOL (Bausch & Lomb) that was studied in 2013 has a

hardness of 11.0 MPa, which was thought to be beneficial because it would prevent scratching and deformation. For comparison, the AcrySof (Alcon Laboratories), Acryfold (Hoya), and Sensar (Abbott Medical Optics) have a surface hardness of 0.24 MPa, 0.68 MPa, and 0.43 MPa, respectively (Packer et al, 2013).

This project's key objective is to synthesize polymers to identify the optimal mechanical properties for an intraocular lens to prevent attachment and proliferation of lens epithelial cells. It is hypothesized that there is a range of elastic moduli that are lower than that of the native lens capsule that help prevent the adhesion of cells and the subsequent epithelial to mesenchymal cell transition. Preventing this cell attachment and transition would be a vital step in preventing posterior capsular opacification by designing improved implants for cataract surgery.

# Methods

*Polymer Synthesis*

3-Methacryloxypropyltris(trimethylsiloxy)silane (TRIS) (Silar), methyl methacrylate (MMA) (Sigma Aldrich), and 2-hydroxyethyl methacrylate (HEMA) (Monomer-Polymer) were copolymerized in a variety of molar ratios using free radical polymerization. The structures of these monomers are shown in Figure 5, below.

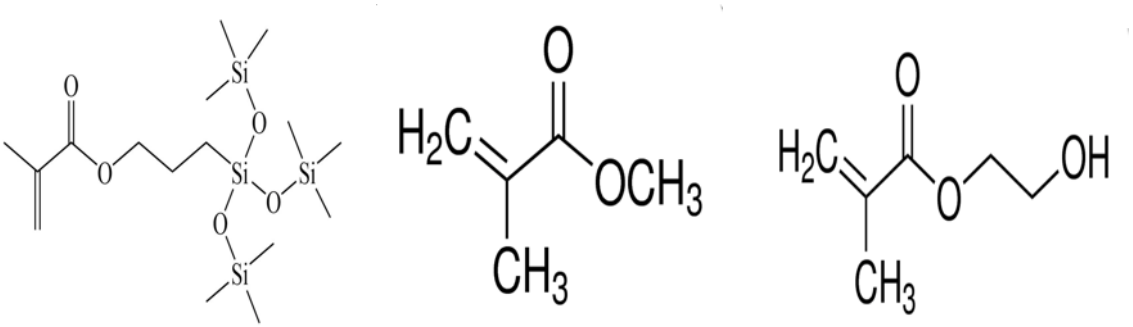


**Figure 5: Structures for TRIS, MMA, and HEMA**

These monomers were selected because they are readily used in contact lenses and intraocular lenses, so they provide clinical relevance (Princz, Lasowski, & Sheardown, 2016). Table 1, on the next page, summarizes all of the polymer compounds synthesized.

**Table 1: List of copolymerized compounds synthesized for testing**

| Label | Monomer 1 & Ratio | Monomer 2 & Ratio |
|---|---|---|
| A | 1 TRIS | - |
| B | 3 TRIS | 1 HEMA |
| C | 2 TRIS | 1 HEMA |
| D | 1 TRIS | 1 HEMA |
| E | 1 TRIS | 2 HEMA |
| F | 1 TRIS | 3 HEMA |
| G | 1 HEMA | - |
| H | 3 TRIS | 1 MMA |
| I | 2 TRIS | 1 MMA |
| J | 1 TRIS | 1 MMA |
| K | 1 TRIS | 2 MMA |
| L | 1 TRIS | 3 MMA |

TRIS compounds including crosslinked dimers were also synthesized. These compounds are summarized in Table 2, below.

**Table 2: List of crosslinked TRIS compounds with dimer for testing**

| Label | Monomer | % Dimer |
|---|---|---|
| M | TRIS | 1 |
| N | TRIS | 2 |
| O | TRIS | 3 |
| P | TRIS | 4 |
| Q | TRIS | 5 |

A 1.5% w/w solution of Vazo 67 (Monomer-Polymer & Dajac Labs) in isopropanol (Fisher Chemical) or isooctane (Fisher Chemical) was used as the initiator. The reaction was run for 6 hours at 70°C in an oil bath after being purged for 2 minutes with nitrogen gas.

After the reaction, the polymers were precipitated in 10-fold excess water or ratios of methanol-water. The wash was changed 5 times to purify and remove any residual monomers. Then, the polymers were heated several times to evaporate all solvent. The final copolymerized samples were dissolved in isopropanol or isooctane as a 7.5% w/w polymer solution in order to later be cast as films or molded.

*Cell Culture*

Preliminary studies were conducted using primary canine lens epithelial cells. After growing the cells in standard culture conditions, they were seeded onto wells of tissue culture plates that were coated with the polymers. Phase contrast microscopy was used to evaluate cell adhesion and proliferation every 24 hours for 7 days.

B3 (ATCC© CRL-11421)™ human lens epithelial cells were obtained and cultured according to the provided protocols. Cells were cultured in Dulbecco's Minimal Essential Medium (DMEM, Gibco) supplemented with 20% fetal bovine serum (Gibco) and 1% Penicillin-Streptomycin (Sigma-Aldrich). They were kept in an incubator at 37°C and an enriched atmosphere of 5% carbon dioxide. The culture medium was replaced every two days.

*Microscopy*

50 µL of each 7.5% w/w polymer solution was deposited onto a glass slide. The slides were left to dry in a fume hood overnight before imaging. They were then sputter coated using a Hummer VI Tabletop Sputter Coater in order for them to be visible with

the scanning electron microscope (SEM). The polymer films were imaged using a Hitachi S-3000H Scanning Electron Microscope to examine the surface.

Polymer films were also created within wells of a sterile 12-well plate. 100 µL of each 7.5% w/w polymer solution was deposited into a different well and left to dry for at least 24 hours. There were a total of 17 different wells, including the control. The cells were then seeded onto the plate at a concentration of $0.5 * 10^6$ cells/mL. The cells were also seeded onto a well without a film in order to provide an untreated control. The cells were then imaged using confocal microscopy at 10x magnification on days 1 and 3. Images were examined for cell density, attachment, and proliferation.

*Mechanical Testing*

Polymer films were cast on glass slides in 50 µL volumes and left to dry overnight. They were then tested using a MTS NanoIndenter XP with TestWorks 4 software. The Delta X and Y for finding the surface were set at -10 µm with an allowable drift rate of 0.2 nm/s. The surface approach distance was default at 1000 nm with an approach velocity of 10 nm/s and an approach sensitivity of 25%. The depth limit was set to 500 nm with a settle time of 25 seconds. The drift determination time was 50 seconds, and the peak hold time was 30 seconds. The frequency set point was 45 Hz. One- way ANOVA analysis was completed on this data in Minitab in order to determine statistical significance.

Rheology was also used to test the mechanical properties of the polymer films. 300 µL of the polymer solution was deposited onto the lower geometry of the parallel

plate rheometer (Malvern Kinexus pro+) and then left to dry for 30 minutes before testing. A strain sweep test from 0.01 to 10% strain was first performed at 1 Hz in order to determine the linear viscoelastic region. The linear region was determined to be in the 0.1% to 1% strain range, so strain sweeps were performed in this range at physiological temperature (37°C) and 1 Hz in order to determine storage and loss modulus.

*Cell Assays*

An MTS assay (Abcam) was used on the cell solutions placed in the well plates to measure cell viability on day 3. This assay is composed of 3-(4,5-dimethyl-2-thiazolyl)-2, 5-diphenyl-2H-tetrazolium bromide, which is reduced by viable cells and then creates a colored formazan dye that can be quantified by measuring the absorbance of the solutions. 100 µL of MTS reagent was added to each well of the plate containing cells seeded on the polymer. Each well plate was then placed in the incubator at 37°C for 2 hours. After 2 hours, 220 µL of solution from each well was transferred to a 96-well plate. This was replicated 3 times for each sample for a total of 24 wells in the 96-well plate. The absorbance was then measured using a SpectraMax M5 plate reader at 490 nm. The average absorbance for each polymer was measured, then it was divided by the average absorbance for the control well and multiplied by 100. A graph was then created by plotting these calculated viability percentages against the average absorbance for each polymer.

## Results and Discussion

*Microscopy: SEM*

SEM images of polymer films were taken to examine the surface. It was somewhat difficult to image some of the polymers because there were not many surface characteristics for the microscope to focus on. Images can be seen below, in Figure 6 and Figure 7.

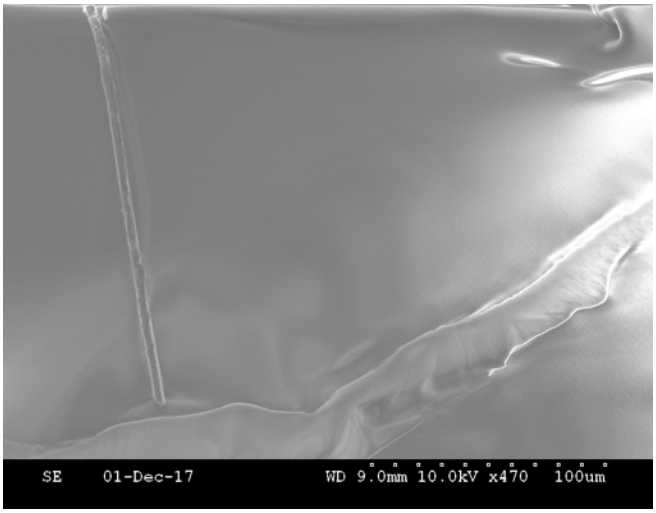


**Figure 6: 2:1 TRIS:MMA imaged with scanning electron microscope**

The polymers looked to be relatively smooth aside from their edges. Some ripples and rivets were present on the surface, most likely from the airflow in the fume hood during casting and drying of the polymer films.

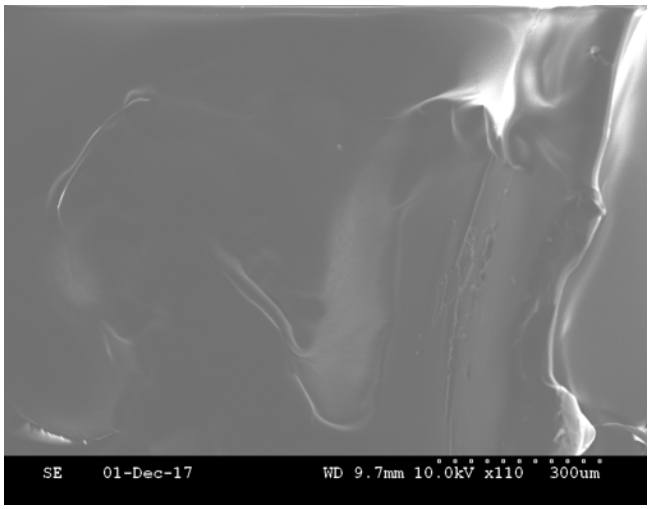


**Figure 7: 3:1 TRIS:MMA imaged with scanning electron microscope**

Originally, films were created on the lab benchtop and covered with a container in order to protect them from outside debris and other materials in the lab. However, it was discovered that this method did not prevent dust and other small particles from getting stuck on the surface of the film.

Although casting them and letting them dry in the fume hood was an improvement, it may be beneficial in the future to find better methods that allow for a smoother surface. Casting them within a small washer on the surface of a glass slide would help to ensure a uniform shape and size and possibly improve the smoothness of the surface. Additionally, casting by spin coating in a cleanroom that would have less dust particles and debris present in the air could be helpful.

*Microscopy: Preliminary K9 Lens Epithelial Cell Data*

Preliminary data on cell attachment to the polymers were collected in collaboration with Dr. Heather Chandler in the College of Optometry at The Ohio State

University. Primary canine (K9) lens epithelial cells were seeded onto all polymers except pure poly(HEMA) and any copolymers containing MMA. As the amount of TRIS present increased, there was more cell attachment. Phase contrast microscopy images for the TRIS and HEMA polymers are shown in Figure 8, below. In the figure, the bright spheres are LECs that have not adhered to the culture well and are no longer viable, due to lack of attachment. The more stretched out blurs are cells that have adhered to the polymer and may be starting to undergo the transition to mesenchymal cells.

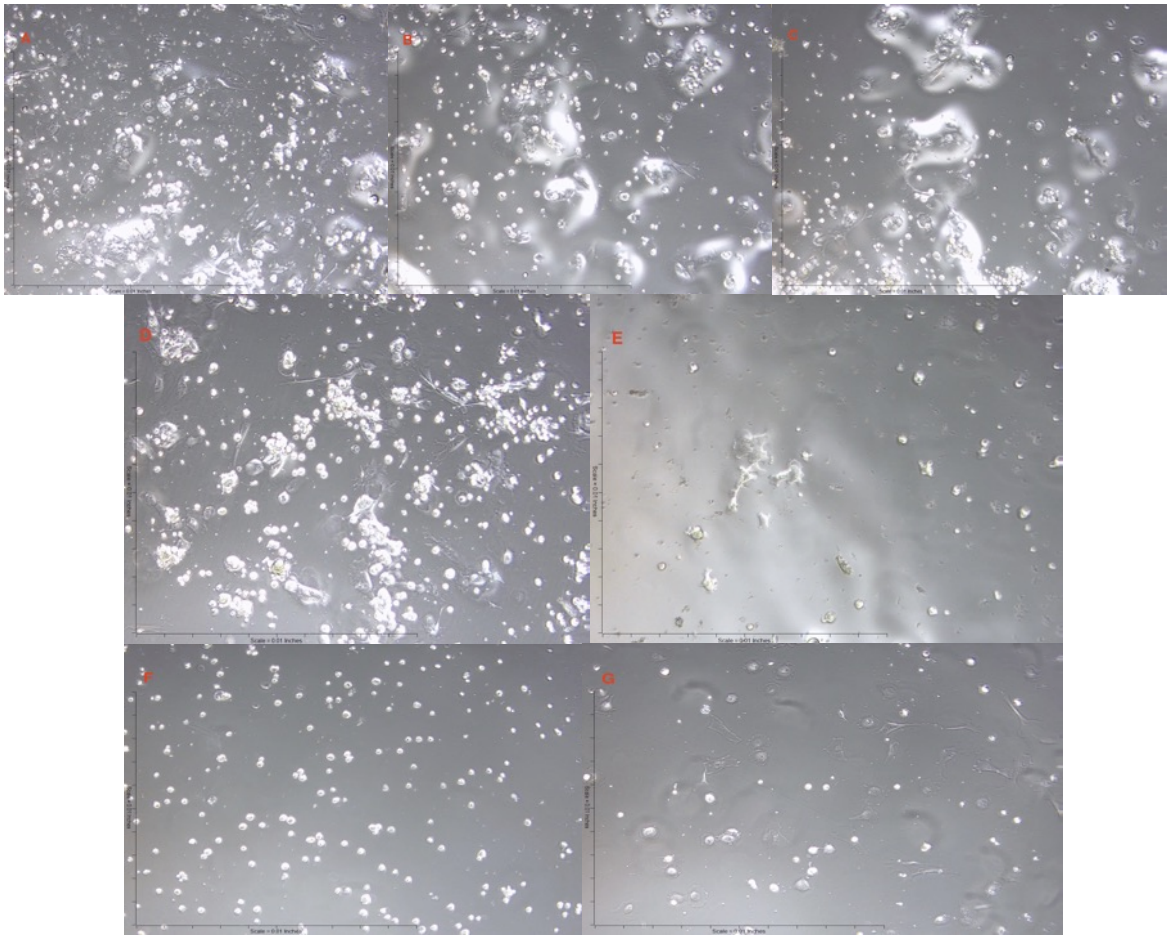


**Figure 8: Phase contrast microscopy for TRIS & HEMA polymers seeded with K9 LECs A) TRIS; B) 3:1 T:H; C) 2:1 T:H; D) 1:1 T:H; E) 1:2 T:H; F) 1:3 T:H; G) Control**

It was concluded that the higher the amount of TRIS in the polymer, the more cell attachment observed. In Figure 8 for the poly(TRIS) sample, many cells are adhered to the polymer surface underneath the non-viable cells. In the sample with the most HEMA (1:3 TRIS:HEMA), there are no cells attached in the background. This study was primarily conducted to look at the effect of amphiphilicity on the amount of cell attachment. The ratio between TRIS and HEMA was changed to change the amphiphilicity because TRIS is more hydrophobic while HEMA is more hydrophilic. It was observed that as the polymers became more hydrophobic, the amount of cell attachment increased.

Based on the hypothesis that less cells would attach to a surface that is less stiff than the lens capsule, it could be hypothesized that TRIS would be stiffer than HEMA. However, when the ratios of copolymerized monomers are varied, the mechanical properties aren't the only thing that is changing and thus aren't the only properties that are affecting the amount of cell attachment. This study focused mainly on creating a range of amphiphilic polymers, but the mechanical properties also could have changed as a result.

Additionally, for the crosslinked polymers, the amount of cell attachment increased as the amount of crosslinking increased. Theoretically, as the amount of crosslinking increases, the modulus should increase as well. This can be seen in Figure 9, on the next page.

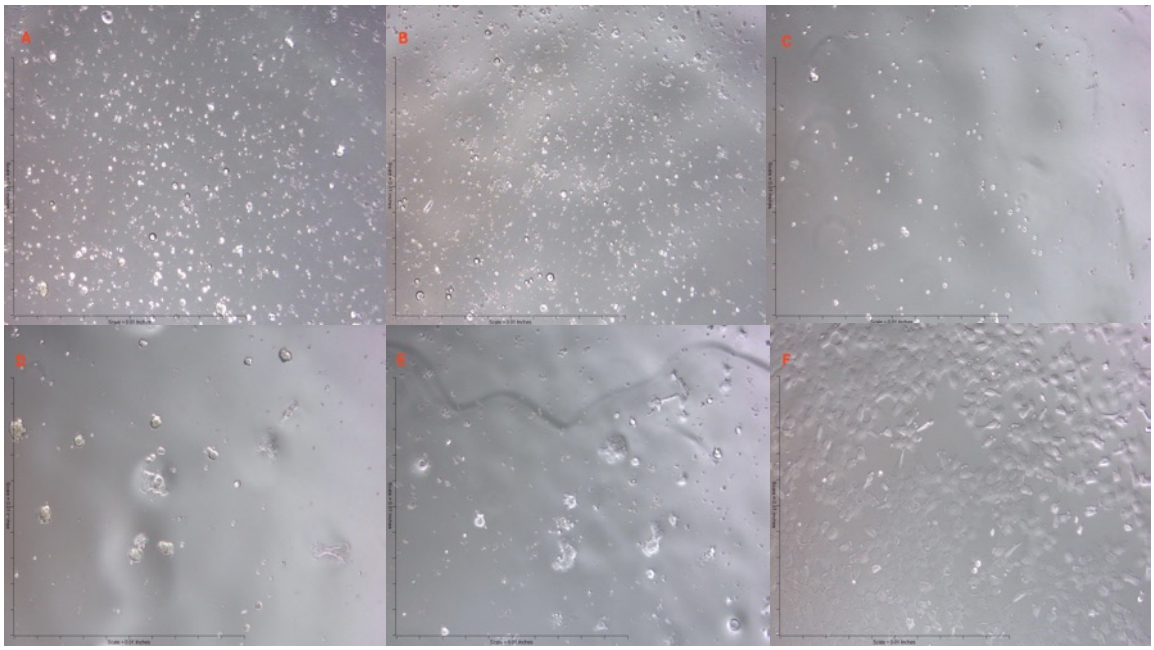

**Figure 9: Phase contrast microscopy images for crosslinked TRIS dimer polymers seeded with K9 LECs. A) 1% dimer; B) 2% dimer; C) 3% dimer; D) 4% dimer; E) 5% dimer; F) control well with no polymer coating**

This data is consistent with the hypothesis that IOLs should be less stiff than the native lens capsule because LECs seem to preferentially attach onto stiffer surfaces. Within the scope of this project, less cell attachment is desired because adhesion on the implant leads to the epithelial-mesenchymal transition and as a result, posterior capsule opacification. According to this preliminary data, there is a trend shown that less stiff surfaces prevent cell adhesion, but future studies need to be conducted to further validate that less stiff IOLs could potentially be successful in preventing LEC adhesion.

The data for the crosslinked TRIS polymers is more conclusive because the only factor that is changing is the amount of crosslinking. With the TRIS/HEMA copolymers, not only are the mechanical properties of each polymer changing, but the surface properties are also changing. TRIS is more hydrophobic than HEMA, which could be affecting cell attachment. It would be beneficial to do a study in which HEMA was tested

with different degrees of crosslinking to see how changing only the mechanical properties for this monomer affects the degree of cell attachment.

This data obviously has some limitations because these cells are not entirely indicative of cell behavior within the lens capsule after phacoemulsification. While lens epithelial cells were used, they were canine cells rather than human cells. Additionally, these results were meant to be preliminary data and weren't necessarily replicated in large sample sizes.

*Microscopy: Primary Lens Epithelial Cell Data*

Data was collected using confocal microscopy on days 1 and 3. The images shown in this section are from day 3. For the TRIS/HEMA polymers, the only wells that exhibited significant cell attachment were the TRIS and the control well. This can be seen in Figure 10, on the next page. While this data did somewhat follow the trend of the preliminary cell studies with canine LECs, it seemed like there was still very little cell attachment on the 3:1 TRIS:HEMA and 2:1 TRIS:HEMA. In the earlier study, there was some cell attachment on these polymers. In the future, it would be helpful to test these polymers in multiple replicates with polymers from a few different batches.

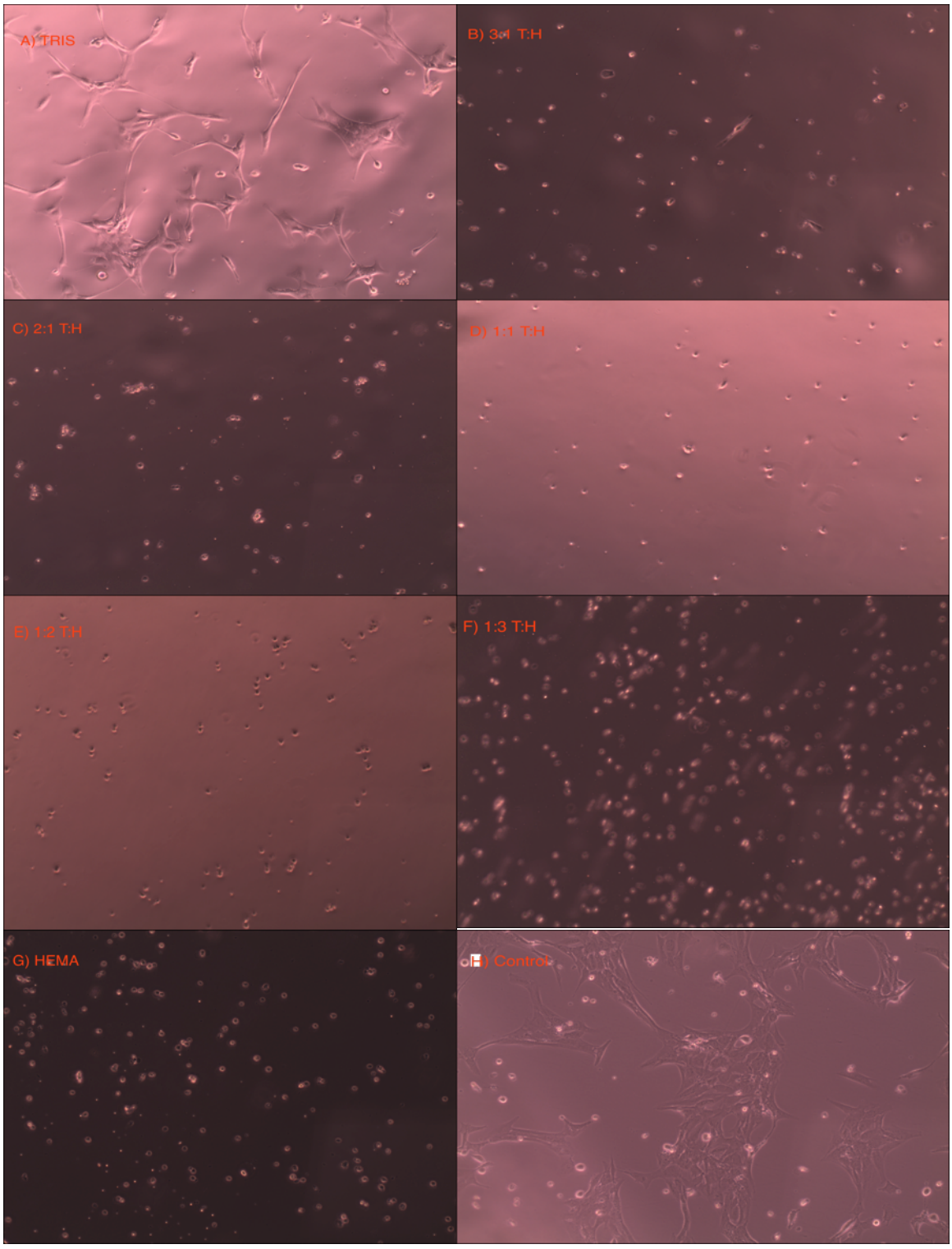


**Figure 10: Confocal microscopy of TRIS/HEMA polymer films seeded with human LECs. A) TRIS; B) 3:1 T:H; C) 2:1 T:H; D) 1:1 T:H; E) 1:2 T:H; F) 1:3 T:H; G) HEMA; H) Control**

The day 3 microscopy pictures for the TRIS/MMA polymers are shown in Figure 11, below.

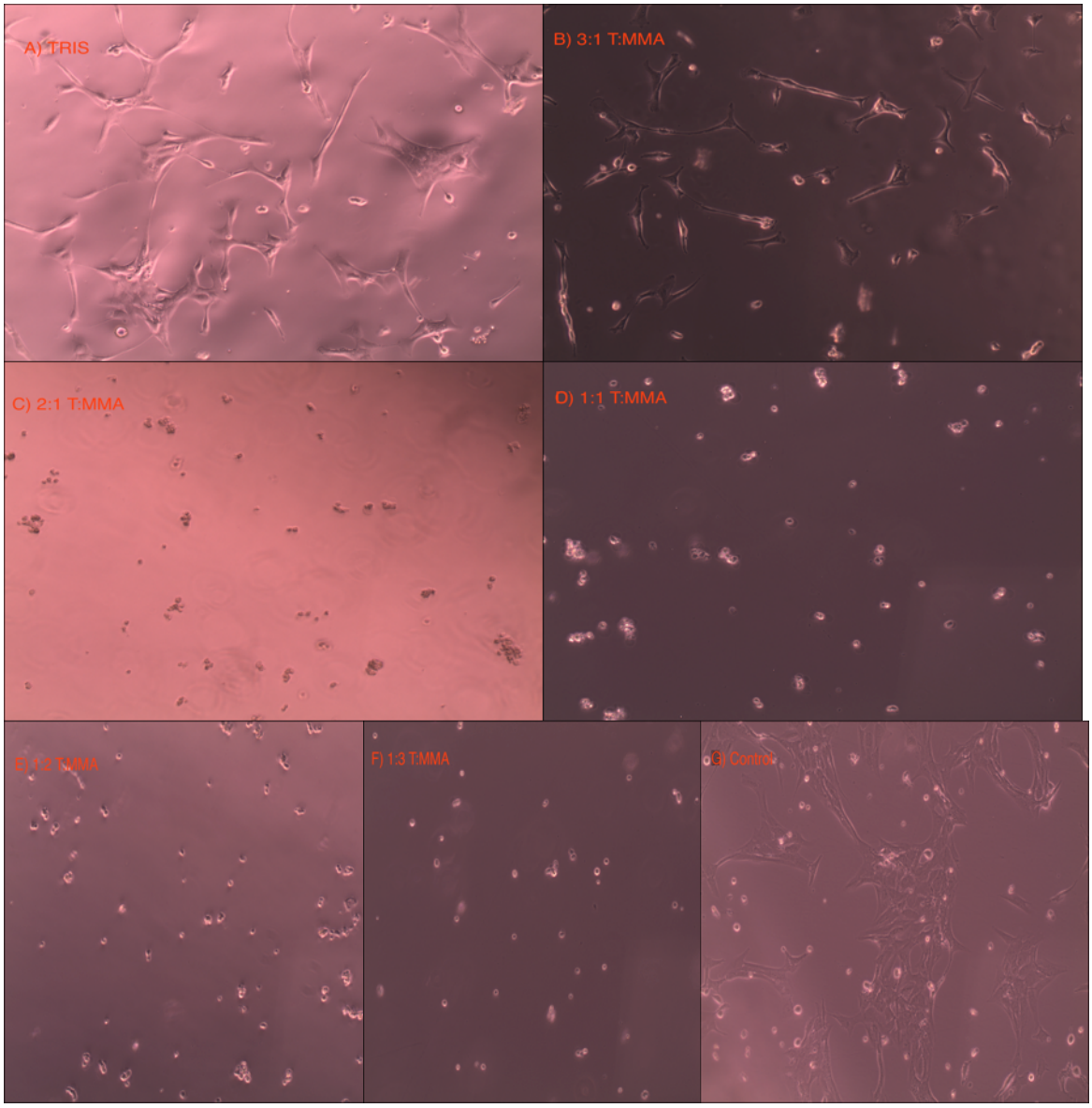


**Figure 11: Confocal microscopy for TRIS/MMA polymer films seeded with human LECs. A) TRIS; B) 3:1 T:MMA; C) 2:1 T:MMA; D) 1:1 T:MMA; E) 1:2 T:MMA; F) 1:3 T:MMA G) Control**

The amount of cell attachment again decreased as the amount of TRIS in the polymers decreased. There was only significant cell attachment on the TRIS, the 3:1 TRIS:MMA, and the control well. There did not seem to be any cell attachment on the polymer films

with a higher ratio of MMA present. The microscopy images for the crosslinked TRIS polymers are shown in Figure 12, below.

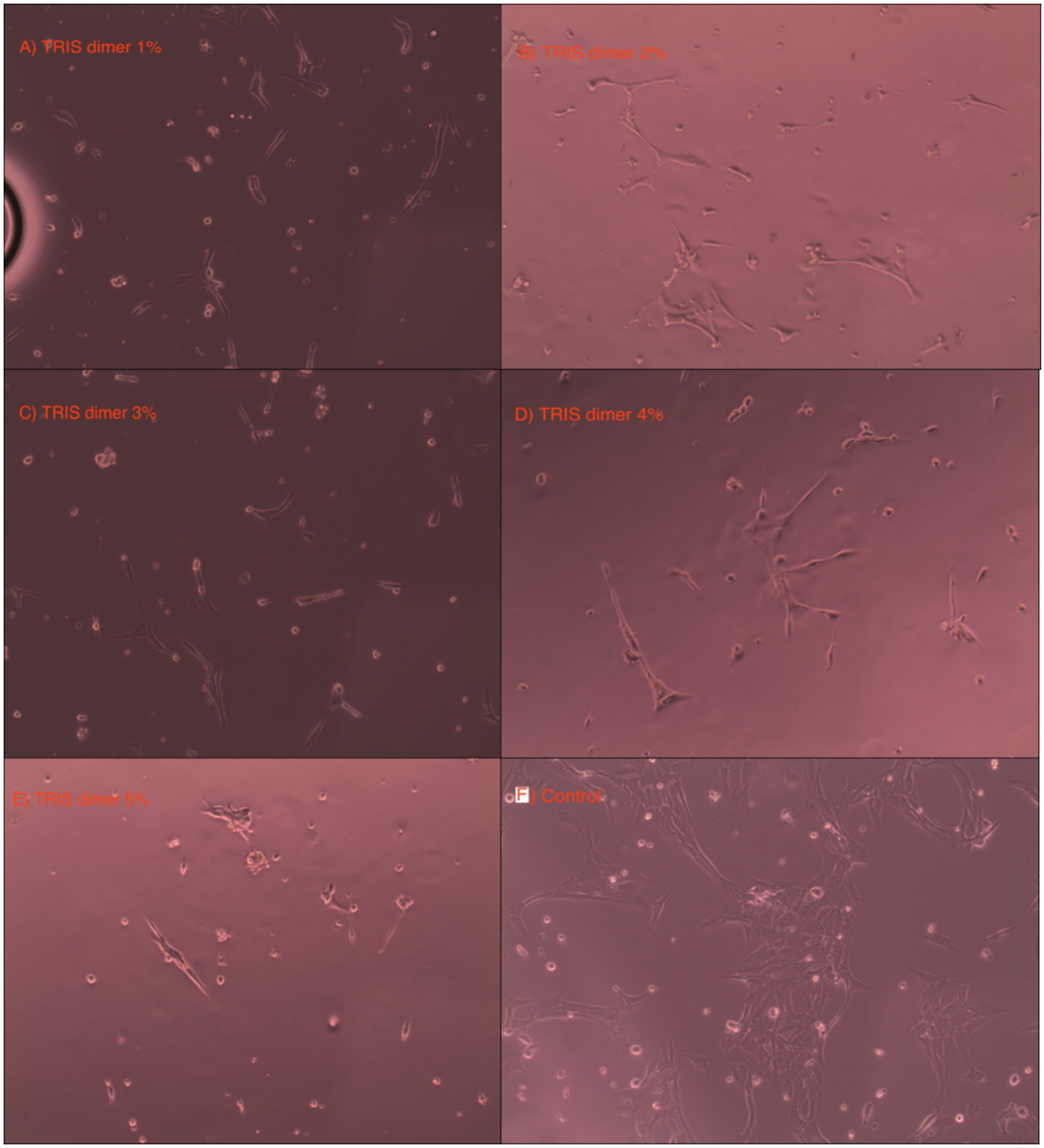


**Figure 12: Confocal microscopy of crosslinked TRIS polymer films seeded with human LECs. A) TRIS dimer 1%; B) TRIS dimer 2%; C) TRIS dimer 3%; D) TRIS dimer 4%; E) TRIS dimer 5%; F) Control**

While all of the crosslinked TRIS polymers had some cells attached, it was difficult to determine which polymers had the most cells attached based solely on microscopy. The MTS assay that was completed was a better way to quantify the cell viability.

*Mechanical Testing*

In nanonindentation, the unloading modulus is taken from the stress-strain curve that is generated as the tip of the nanoindenter unloads all of the stress it was exerting on the sample. The unloading line is parallel with the linear part of the initial stress-strain diagram. Because of this, the slopes of the two lines are estimated to be about the same, and thus, the modulus can be estimated based on the slope of the unloading line. This slope is the unloading modulus. Table 3, below, summarizes the unloading modulus acquired for the samples that were testable by nanoindentation.

**Table 3: Mean unloading moduli and standard deviation for samples testable with MTS Nanoindenter XP**

| Label | Polymer Description | Mean Unloading Modulus (GPa) | Standard Deviation |
|---|---|---|---|
| A | TRIS | 12.65 | 0.19 |
| E | 1:2 T:H | 1.67 | 0.18 |
| F | 1:3 T:H | 1.80 | 0.03 |
| M | TRIS Dimer 1% | 8.74 | 7.30 |
| N | TRIS Dimer 2% | 25.41 | - |

However, nanoindentation had some limitations and was relatively inconclusive for certain samples. A one-way ANOVA analysis was done on the nanoindentation data. The boxplot from this analysis is shown in Figure 13, on the next page.

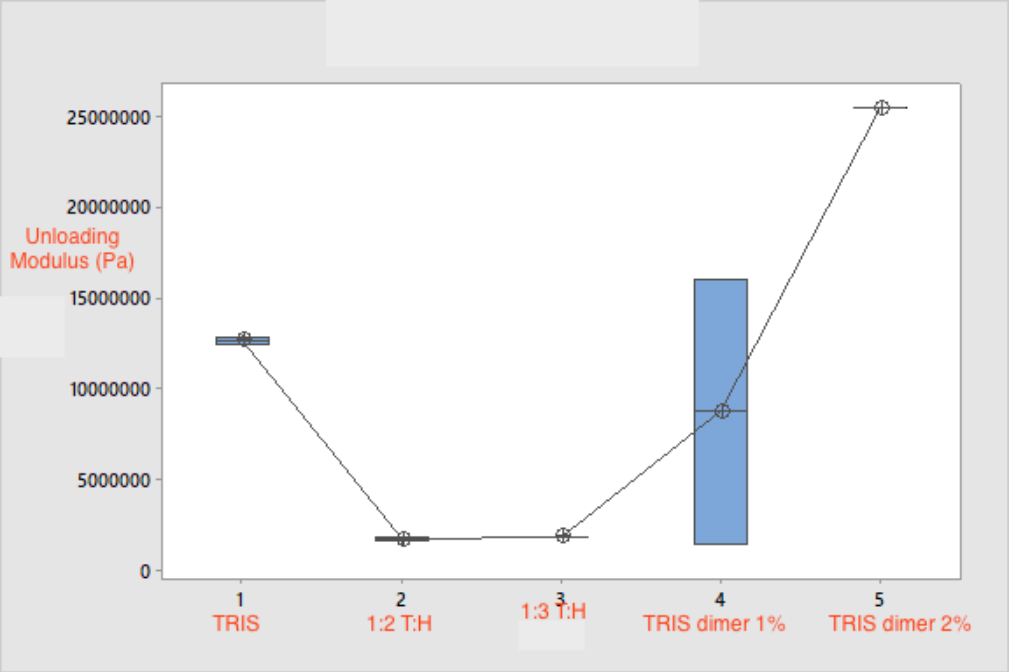


**Figure 13: Boxplot for one-way ANOVA run on nanoindentation data**

With high standard deviations and unloading moduli that were 2 orders of magnitude above what was expected, this data was thought to be incorrect. Many of the samples did not dry in a film that was flat enough for the nanoindenter to test properly. Performing nanoindentation on polymers still involves several experimental difficulties. This technique is usually used on harder materials such as metals and ceramics (Tranchida & Piccarolo, 2005). Because of all of these reasons, it was decided that rheology would be a better method to test the mechanical properties of the polymers.

After the strain sweep was conducted at 1 Hz, it was the linear viscoelastic region was in the range from 0.1% to 1% strain. From this test, the average storage modulus (G') and average loss modulus (G'') as well as standard deviation could be calculated. An example of the plot generated from the strain sweep rheology test can be seen in Figure 14, on the next page.

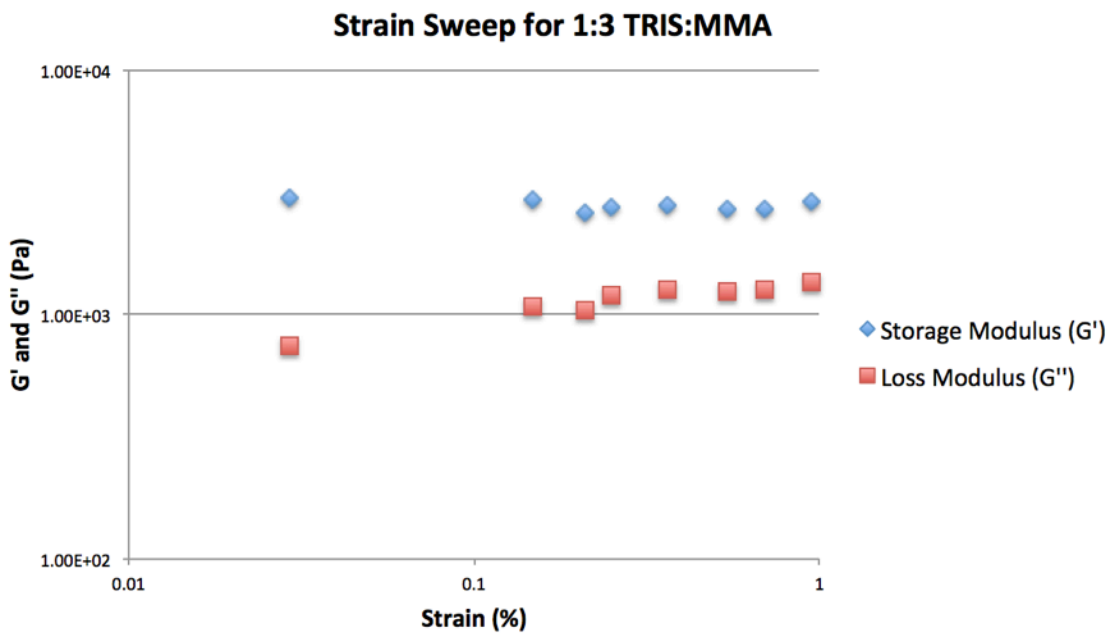


**Figure 14: Determination of linear region for polymers using 0.1%-1% strain sweep of 1:3 TRIS:MMA**

This trend stayed relatively consistent for all of the different polymers. The moduli were in the kPa range, which is in the same order of magnitude as the native lens capsule's modulus, which has been measured in the range of 400-1500 kPa (Krag & Andreassen, 2003). Table 4, on the next page, summarizes the data that was collected in the rheology strain sweep tests for elastic moduli and viscous moduli of the copolymers.

**Table 4: Storage modulus (G') and loss modulus (G'') measured from strain sweep rheology testing for copolymerized monomers**

| Label | Monomer 1 & Ratio | Monomer 2 & Ratio | Average G' (kPa) | Standard Deviation | Average G'' (kPa) | Standard Deviation |
|---|---|---|---|---|---|---|
| A | 1 TRIS | - | 3.65 | 0.143 | 2.17 | 0.108 |
| B | 3 TRIS | 1 HEMA | 3.61 | 0.188 | 1.98 | 0.199 |
| C | 2 TRIS | 1 HEMA | 4.16 | 0.408 | 2.17 | 0.190 |
| D | 1 TRIS | 1 HEMA | 2.65 | 0.678 | 0.452 | 0.652 |
| E | 1 TRIS | 2 HEMA | 4.13 | 1.22 | 0.983 | 0.584 |
| F | 1 TRIS | 3 HEMA | 2.18 | 0.802 | 0.121 | 0.041 |
| G | 1 HEMA | - | 0.952 | 0.121 | 0.823 | 0.137 |
| H | 3 TRIS | 1 MMA | 13.7 | 1.954 | 33.4 | 4.573 |
| I | 2 TRIS | 1 MMA | 4.67 | 0.291 | 4.56 | 0.270 |
| J | 1 TRIS | 1 MMA | 29.8 | 4.965 | 32.6 | 6.532 |
| K | 1 TRIS | 2 MMA | 1.74 | 0.238 | 0.270 | 0.087 |
| L | 1 TRIS | 3 MMA | 2.79 | 0.126 | 1.14 | 0.179 |

This data can also be visualized in the plots below that show the strain versus stiffness for rheology tests. The data for the TRIS/HEMA polymers are shown in Figure 15, on the next page. This plot shows TRIS is stiffer than HEMA, and supports the hypothesis that stiffer surfaces may influence cell attachment because it had more cells that attached to it. Overall, its surface properties as well as mechanical properties may tend to promote more cell adhesion. HEMA, which had less cells adhered to it when it was in higher quantity in the preliminary studies, was measured to be the least stiff out of all of the TRIS/HEMA polymers. This stiffness, in addition to its preferential surface energy, may have contributed to the lack of cell attachment. According to these trends, it could be hypothesized that HEMA would be better for IOL materials than TRIS based on substrate stiffness or surface chemistry.

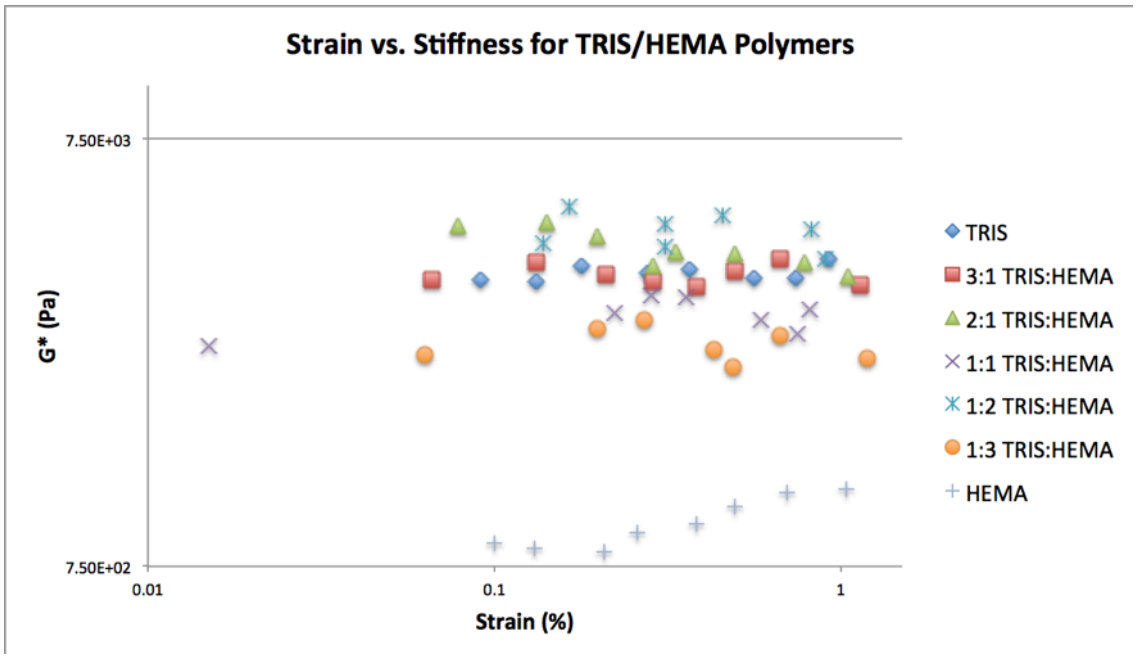


**Figure 15: Strain versus stiffness plot for rheology of TRIS/HEMA polymers**

A one-way ANOVA test was run on this data in Minitab to determine the statistical significance. The resulting boxplot from the test are in Figure 16, below.

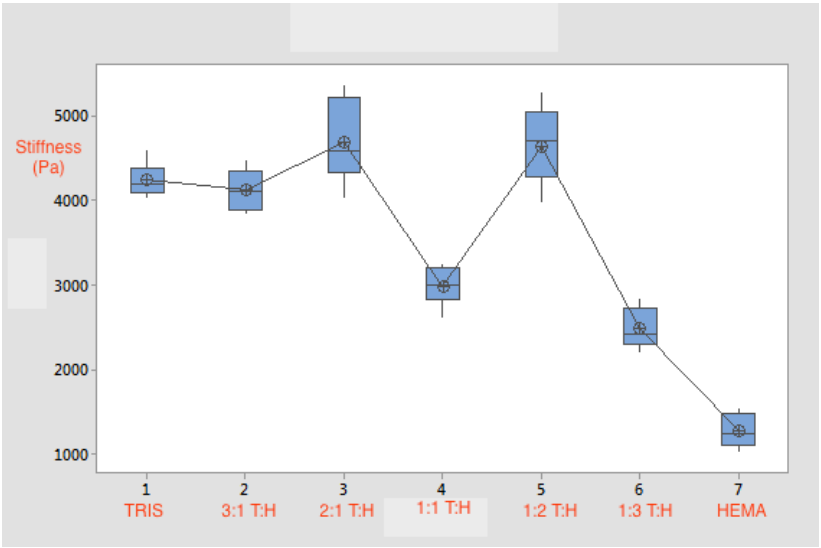


**Figure 16: Boxplot from one-way ANOVA test of TRIS/HEMA polymers to determine statistical significance**

This boxplot shows whether or not samples had statistically different stiffnesses. One thing to note is that the stiffness for the TRIS and the HEMA were significantly different. This supports the earlier stated hypothesis that TRIS had more cell attachment in cell studies not only because of its preferential surface energy, but also because of its preferential stiffness. However, the TRIS had much more cell attachment than any of the other polymers despite the fact that it was only statistically different from 1:1 TRIS:HEMA, 1:3 TRIS:HEMA, and HEMA. This is most likely because the changing surface energy was influencing the amount of cell attachment as well.

The data for the TRIS/MMA polymer stiffness is shown in Figure 17, below.

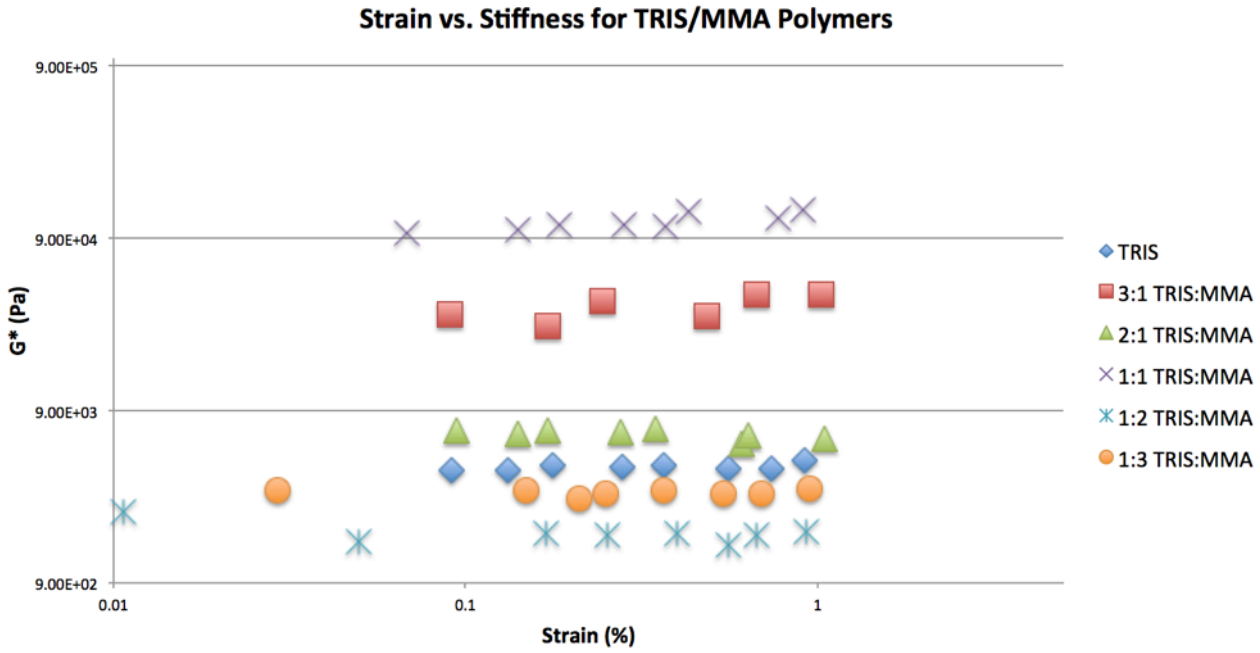


**Figure 17: Strain versus stiffness plot for rheology of TRIS/MMA polymers**

In relation to these polymers, the most stiff sample was the 1:1 TRIS:MMA. The stiffness did not follow any concrete trends when the ratio of TRIS:MMA was changing.

It appears that the stiffness may increase as the amount of TRIS in the copolymer increases, but the poly(TRIS) is not the stiffest polymer.

Statistical analysis was also completed on the stiffness of these polymers. A one-way ANOVA test in Minitab was run in order to determine the statistical significance. The box plot shown in Figure 18, below, is representative of this test for the TRIS/MMA polymers.

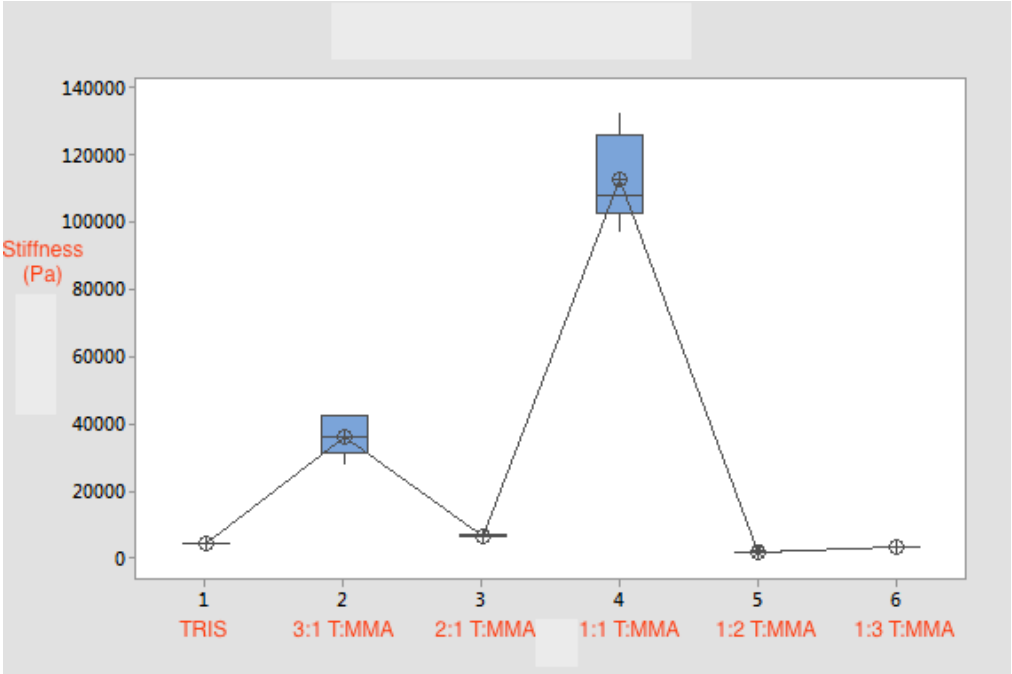


**Figure 18: Box plot from one-way ANOVA test for TRIS/MMA polymers to determine statistical significance**

The only two samples that we determined to be statistically different from the other samples as well as each other were the 3:1 TRIS:MMA and the 1:1 TRIS:MMA. This data seems to be somewhat random and doesn't really follow a trend as the ratios change. The 3:1 TRIS:MMA had a significant amount of cell attachment, which could potentially be contributed to its higher stiffness. However, the 1:1 TRIS:MMA had

virtually no cell attachment despite its high stiffness in comparison to the other TRIS/MMA polymers.

This could be contributed to its surface energy or other properties that could inhibit cell attachment. It would be beneficial to study the surface energy of polymers involving MMA to examine this. Future studies should be done in order to provide more concrete trends for the mechanical properties of these polymers. More replicates of each rheology trial should be performed, and rheological methods should be fine-tuned, which will be discussed later.

Rheology data were also collected for the crosslinked TRIS polymers. This is shown in Table 5, below.

**Table 5: Storage modulus (G') and loss modulus (G'') measured from strain sweep rheology testing for copolymerized monomers**

| Label | Monomer | % Dimer | Average G' (kPa) | Standard Deviation | Average G'' (kPa) | Standard Deviation |
|---|---|---|---|---|---|---|
| M | TRIS | 1 | 2.63 | 0.149 | 0.326 | 0.104 |
| N | TRIS | 2 | 1.43 | 0.281 | 0.984 | 0.210 |
| O | TRIS | 3 | 2.03 | 0.163 | 0.266 | 0.059 |
| P | TRIS | 4 | 2.91 | 0.277 | 1.38 | 0.127 |
| Q | TRIS | 5 | 2.61 | 0.465 | 2.37 | 0.695 |

A graph of the strain versus measured stiffness (G*) is shown in Figure 19, on the next page. This visual representation demonstrates that the polymer with the least amount of crosslinking was not the least stiff, which was unexpected. While the general trend does follow the expected results that the more crosslinking there is, the more stiff the polymer will be, there are some limitations or errors with this data that should be corrected in future work.

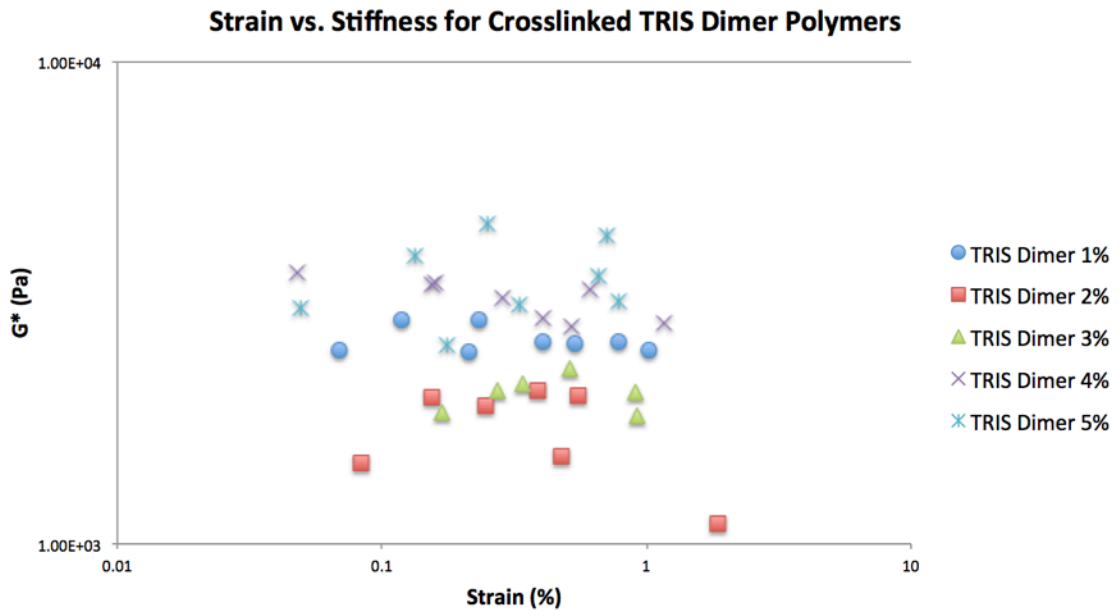


**Figure 19: Strain vs. stiffness scatter plot for rheology of crosslinked TRIS dimer polymers**

It is clear that the measured mechanical properties of the crosslinked TRIS polymers don't follow the expected trends. As the degree of crosslinking increases, the polymer should be stiffer and thus have a higher modulus and stiffness measured. The data gathered from rheology doesn't match up with this. While the most crosslinked polymer does have the highest stiffness, the least crosslinked polymer was also measured to have a stiffness that was just as high as the 3% and 4% crosslinked polymer. However, all of these stiffnesses were still below that of the native lens capsule.

A one-way ANOVA test was run on the stiffness measurements for the crosslinked TRIS polymers in order to determine if there was any statistical significance. The box plot that was generated from this test is shown in Figure 20, on the next page.

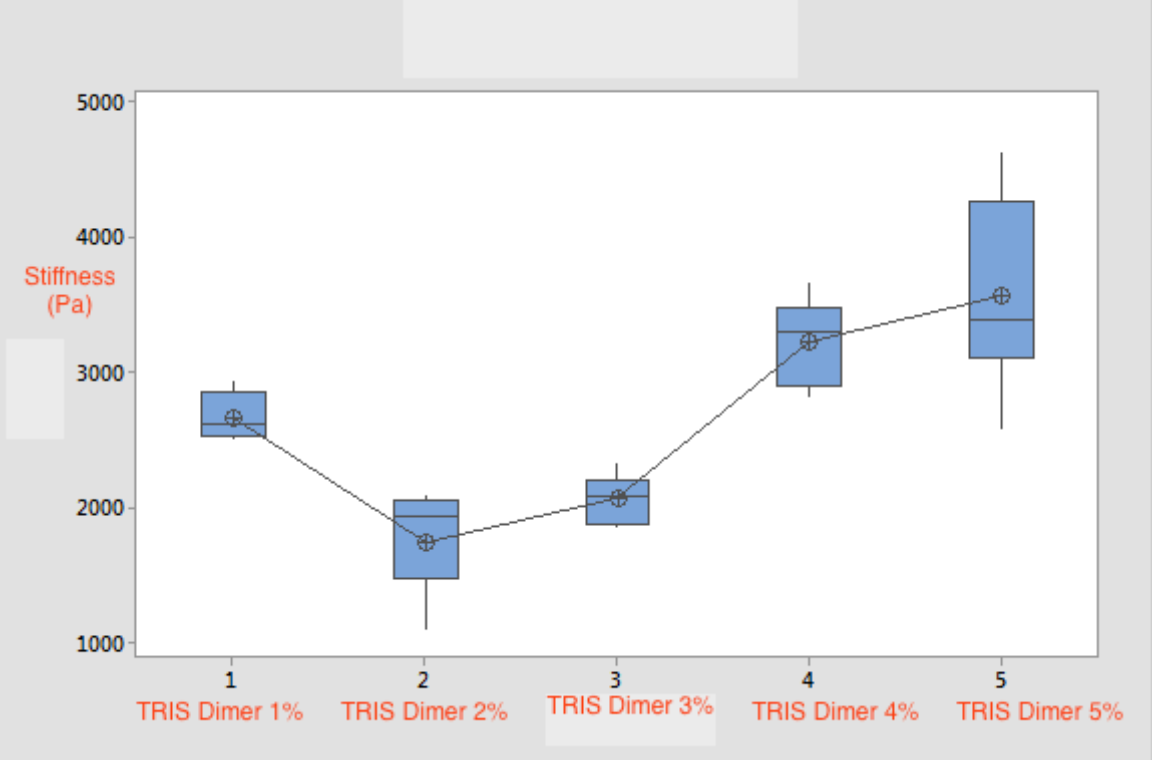


**Figure 20: Boxplot from one-way ANOVA test to determine statistical significance of TRIS dimer stiffnesses**

The ANOVA test and subsequent Tukey test showed that most of the samples were statistically different from one another if they varied more than 1% in the amount of crosslinking. The only exception was that the 1% crosslinker was not statistically different from the 3% or 4% crosslinker. This was expected, as the 1% crosslinker seemed to be an outlier.

In order to ensure more accurate measurements are taken in the future, some changes to the rheology procedure should be changed. Instead of doing a strain sweep, it may be more beneficial to run this test at a constant strain rate and generate a stress-strain curve in order to calculate the modulus. Additionally, it would be helpful to create a mold or boundary that would let the sample dry in a uniform shape and size each time. Sometimes the molded samples did not seem completely dry, smooth, or homogenous.

This could have affected the data, so in the future, creating a more consistent and uniform mold would be beneficial in getting accurate data.

*Cell Assays*

The MTS assay was run on all polymers samples in order to determine the cell viability within the well plates. The viability was calculated as a percent of the control well, which was treated as 100% viability and had no polymer in it. Figure 21, below, shows the viability for the TRIS/HEMA polymers. The TRIS had much more viable cells than all of the other polymers, which was evident in the microscopy as well. This trend was expected based on the hypothesis that stiffer surfaces would have more cells adhered to them, but the other amphiphilic polymers did not follow this trend.

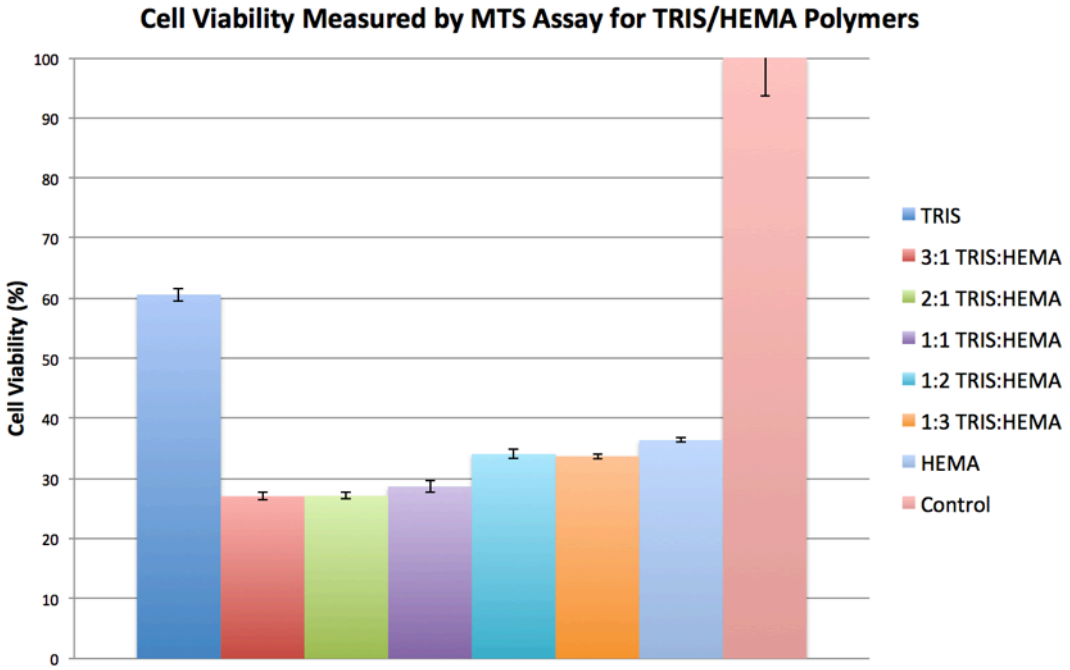


**Figure 21: Cell viability data for TRIS/HEMA polymers**

For the TRIS/MMA polymers, a similar trend was exhibited. The TRIS had the highest amount of cell viability. Based on the hypothesis that stiffer polymers promote cell adhesion more and the mechanical testing results, the 3:1 TRIS:MMA and 1:1 TRIS:MMA should have significantly more cell viability because they are significantly more stiff. However, the TRIS still had a higher cell viability despite the fact that it was statistically lower for its measured mechanical properties. This data is a bit inconsistent, but 3:1 TRIS:MMA and 1:1 TRIS:MMA still both have the highest cell viability percentage after TRIS. This can be seen in Figure 22, below.

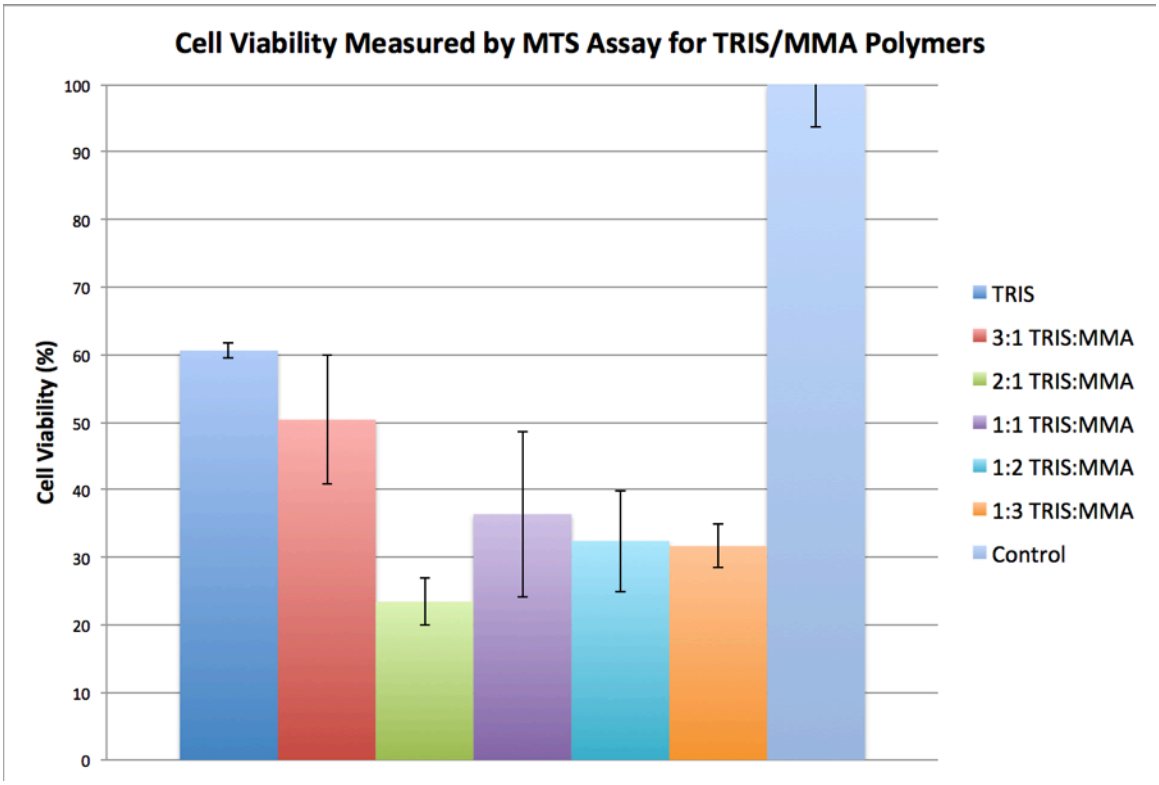


**Figure 22: Cell viability data for TRIS/MMA polymers**

The crosslinked TRIS polymer cell viability is shown on the next page in Figure 23. This assay was important because it was difficult to tell which polymer had the most cells adhered to it based solely on microscopy. The 1% crosslinker had the highest amount of

cell attachment, which did not match up with the hypothesis that a more crosslinked and theoretically stiffer polymer would have more cells adhered to it. This data does not really follow a trend, although all crosslinked polymers did have greater than 40% cell viability. This was the highest for all of the polymers measured in this study. While there were no significant trends followed between the crosslinked polymers themselves, between all of the polymers studied, there was a general trend that TRIS polymers had more cells adhered to them. This suggests that TRIS is probably not ideal for use in IOLs because an ideal IOL would have minimal cell attachment, leading to minimal PCO. However, the cell attachment on TRIS polymers could be due to surface free energy

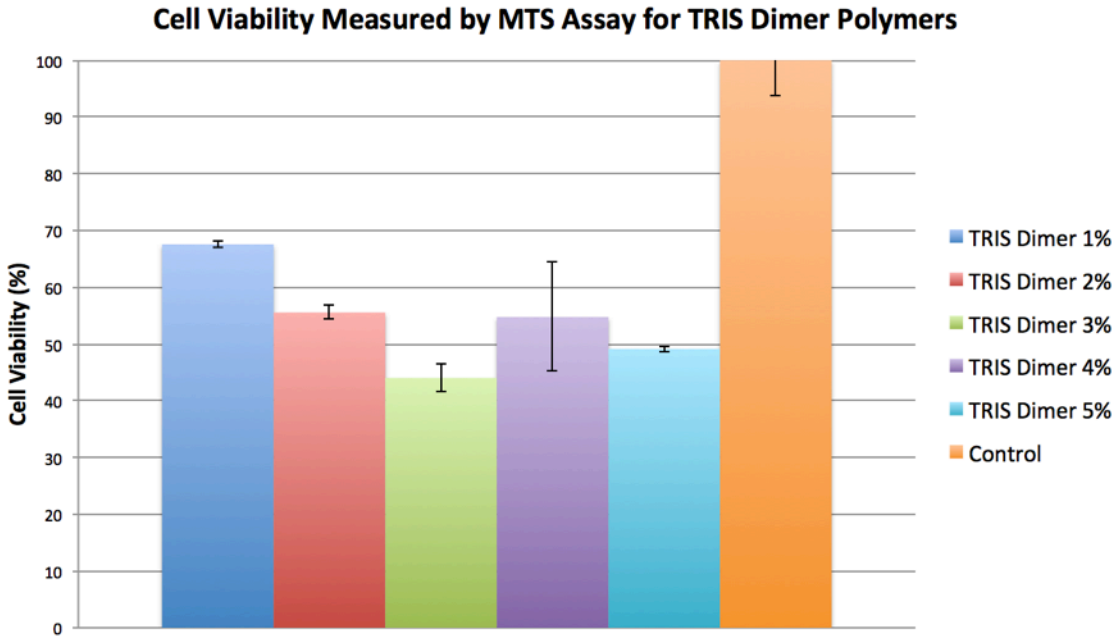


**Figure 23: Cell viability data for crosslinked TRIS polymers**

## Conclusions & Future Studies

Overall, the experimental tests showed that polymers with higher moduli tend to promote cell adhesion. This was consistent with the hypothesis that intraocular lenses with lower mechanical properties than that of the native lens capsule could have less cell attachment and subsequently, less posterior capsular opacification. However, it seems that better methods to characterize the mechanical properties of the polymers are needed. Neither nanoindentation nor rheology data were completely consistent. There were not many clear trends exhibited other than TRIS being measured as stiffer than HEMA and that in general, the mechanical properties of the crosslinked TRIS polymers got stiffer with more crosslinking. These higher moduli could have led to poly(TRIS) having the highest amount of cell attachment, but it also could have been caused by other properties such as surface energy.

It will eventually be necessary to carry out a full-scale characterization of material properties to determine the properties that prevent lens epithelial cell attachment and subsequent transition to mesenchymal cells. This will allow researchers to execute a bottom-up approach in designing intraocular lenses that are the most effective at preventing posterior capsule opacification. While this study mainly focuses on the mechanical properties of potential IOL materials, other properties such as surface energy, shape, and edge design could also have a significant effect on the incidence of PCO after cataract surgery. Our group has previously done a study of the effects of surface energy

of polymers on lens cell attachment and subsequent proliferation. We have found that an intermediate surface energy is preferable to prevent adhesion and proliferation.

Future investigations should be designed to evaluate epithelial cell attachment, proliferation, and transition on a more long-term scale. Secondary cataract can occur 2-5 years after surgery, so short-term *in vitro* studies may not be completely indicative of long-term trends. Additionally, *in vivo* studies should be carried out in order to determine larger scale effects. Because this study was limited to cell studies rather than *in vivo* models, this would be an important factor in finding out if these trends hold true *in vivo.*

## Bibliography

Awasthi, N., Guo, S., & Wagner, B. J. (2009). Posterior capsular opacification: a problem reduced but not yet eradicated. *Archives of Ophthalmology,* 127(4):555-562. http://jamanetwork.com/journals/jamaophthalmology/fullarticle/422987

Betrand, V., Bozukova, D., & Lanera, T.S. (2014). Biointerface multiparametric study of intraocular lens acrylic materials. *Journal of Cataract and Refractive Surgery,* 40:1536-1544.

Cunanan, C. M., Tarbaux, N.M., & Knight, P.M. (1991). Surface properties of intraocular lens materials and their influence on in vitro cell adhesion. *Journal of Cataract and Refractive Surgery*, 17:767-773.

Findl, O. Intraocular lens materials and design (2009). *Achieving Excellence in Cataract Surgery*, edited by D. Michael Colvard, 95-108.

Hollick, E.J., Spalton, D. J., Ursell, P. G., Pande, M.V., Barman, S.A., Boyce, J.F. & Tilling, K (1999). The effect of polymethylmethacrylate, silicone, and polyacrylic intraocular lenses on posterior capsular opacification 3 years after cataract surgery. *Ophthamology,* 106:49-55.

Huang, X., Wang, Y., Cai, J., Ma, X., Li, Y., Cheng, J., & Wei, R. (2013). Surface modification of intraocular lenses. *Journal of Ocular Pharmacology and Therapeutics*, 29(2):208-215.

Iwase, T., Nishi, Y., Oveson, B.C., & Jo, Y. (2011). Hydrophobic versus double-square

edged hydrophilic foldable acrylic intraocular lens: effect on posterior capsule opacification. *Journal of Cataract and Refractive Surgery*, 37:1060-1068.

Krag, S., & Andreassen, T.T. (2003). Mechanical properties of the human lens capsule. *Progress in Retinal and Eye Research*, 22:749-767.

Kugelberg, M., Wejde, G., Jayaram, H., & Zetterström, C. (2008). Two-year follow-up of posterior capsule opacification of a hydrophilic or hydrophobic acrylic intraocular lens. *Acta Ophthalmologica*, 86:533-536.

Laser Cataract Surgery. *Southwestern Eye Associates.* Retrieved from http://www.sweye.net/cataracts/laser-cataract-surgery/

Liu, Y. C., Williams, M., Kim, T., Malyugin, B., & Mehta, J.S. (2017). Cataracts. *The Lancet*, 390(11094):600-612.

Menucci, R., Favuzza, E., Boccalini, C., Gicquel, J., & Raimondi, L. (2015). Square-edge intraocular lenses and epithelial lens cell proliferation: implications on posterior capsule opacification in an in vitro model. *BMC Ophthalmology*, 15:5.

Nishi, O., Nishi, K., & Osakabe, Y. (2004). Effect of intraocular lenses on preventing posterior capsule opacification: Design versus material. *Journal of Cataract and Refractive Surgery*, 30:2170-2176.

Oshika, T., Nagata, T., & Ishii, Y. (1998). Adhesion of lens capsule to intraocular lenses of polymethylmethacrylate, silicone, and acrylic foldable materials: an experimental study. *British Journal of Ophthalmology*, 82: 549-553.

Packer, M., Fry, L., Lavery, K.T., Lehmann, R., McDonald, J., Nichamin, L., Bearie, B., Hayashida, J., Altmann, G.E., & Khodai, O. (2013). Safety and effectiveness of a

glistening-free single-piece hydrophobic acrylic intraocular lens (enVista). *Clinical Ophthalmology*, 7:1905-1912.

Princz, M.A., Lasowski, F.J.R., & Sheardown, H. (2016). Advances in intraocular lens materials. *Biomaterials and Regenerative Medicine in Ophthalmology,* edited by T.V. Chirila and D.G. Harkin, Woodhead Publishing, 401-417.

Spalton, D.J. (1999). Posterior capsular opacification after cataract surgery. *Eye*, 13:489 492.

Tortolano, L., Serrano, C., Jubeli, E., Saunier, J., & Yagoubi, N. (2015). Interaction of intraocular lenses with fibronectin and human lens epiethlial cells: Effect of chemical composition and again. *Journal of Biomedical Materials Research,* 103A(12):3843-3851.

Tranchida, D. & Piccarolo, S. (2005). On the use of the nanoindentation unloading curve to measure the Young's Modulus of polymers on a nanometer scale. *Macromolecular Rapid Communications*, 26:1800-1804.

Ursell, P.G., Spalton, D.J., Pande, M.V., Hollick, E.J., Barman, S., Boyce, J., & Tilling, K. (1998). Relationship between intraocular lens biomaterials and posterior capsule opacification. *Journal of Cataract and Refractive Surgery*, 24:352-360.

Versura, P., Torreggiani, A., Cellini, M., & Caramazza, R. (1999). Adhesion mechanisms of human lens epithelial cells on 4 intraocular lens materials. *Journal of Cataract and Refractive Surgery*, 25:527-533.